The Translational Repressor 4E-BP1 Contributes to Diabetes-Induced Visual Dysfunction

William P. Miller,[1] Maria L. Mihailescu,[1] Chen Yang,[1] Alistair J. Barber,[1,2] Scot R. Kimball,[1] Leonard S. Jefferson,[1] and Michael D. Dennis[1]

[1]Department of Cellular and Molecular Physiology, The Pennsylvania State University College of Medicine, Hershey, Pennsylvania, United States
[2]Department of Ophthalmology, The Pennsylvania State University College of Medicine, Hershey, Pennsylvania, United States

Correspondence: Michael D. Dennis, Department of Cellular and Molecular Physiology, H166, The Pennsylvania State University College of Medicine, 500 University Drive, Hershey, PA 17033, USA; mdennis@psu.edu.

Submitted: November 23, 2015
Accepted: February 15, 2016

Citation: Miller WP, Mihailescu ML, Yang C, et al. The translational repressor 4E-BP1 contributes to diabetes-induced visual dysfunction. *Invest Ophthalmol Vis Sci*. 2016;57:1327–1337. DOI:10.1167/iovs.15-18719

Purpose. The translational repressor 4E-BP1 interacts with the mRNA cap-binding protein eIF4E and thereby promotes cap-independent translation of mRNAs encoding proteins that contribute to diabetic retinopathy. Interaction of 4E-BP1 with eIF4E is enhanced in the retina of diabetic rodents, at least in part, as a result of elevated 4E-BP1 protein expression. In the present study, we examined the role of 4E-BP1 in diabetes-induced visual dysfunction, as well as the mechanism whereby hyperglycemia promotes 4E-BP1 expression.

Methods. Nondiabetic and diabetic wild-type and 4E-BP1/2 knockout mice were evaluated for visual function using a virtual optomotor test (Optomotry). Retinas were harvested from nondiabetic and type 1 diabetic mice and analyzed for protein abundance and posttranslational modifications. Similar analyses were performed on cells in culture exposed to hyperglycemic conditions or an *O*-GlcNAcase inhibitor (Thiamet G [TMG]).

Results. Diabetes-induced visual dysfunction was delayed in mice deficient of 4E-BP1/2 as compared to controls. 4E-BP1 protein expression was enhanced by hyperglycemia in the retina of diabetic rodents and by hyperglycemic conditions in retinal cells in culture. A similar elevation in 4E-BP1 expression was observed with TMG. The rate of 4E-BP1 degradation was significantly prolonged by either hyperglycemic conditions or TMG. A PEST motif in the C-terminus of 4E-BP1 regulated polyubiquitination, turnover, and binding of an E3 ubiquitin ligase complex containing CUL3.

Conclusions. The findings support a model whereby elevated 4E-BP1 expression observed in the retina of diabetic rodents is the result of *O*-GlcNAcylation of 4E-BP1 within its PEST motif.

Keywords: diabetes, retina, eukaryotic translation initiation, eukaryotic translation initiation factor 4E-binding protein 1 (EIF4EBP1), ubiquitylation (ubiquitination)

The primary cause of diabetic retinopathy is neurovascular complications that result from hyperglycemia.[1] The Diabetes Control and Complications Trial demonstrated that intensive glycemic control is associated with a reduction in both the onset and progression of diabetic retinopathy,[2] yet the molecular mechanisms of hyperglycemia-mediated neurovascular dysfunction remain incompletely understood. We recently demonstrated that hyperglycemia promotes translation of the mRNA encoding the proangiogenic cytokine vascular endothelial growth factor (VEGF) in the retina of diabetic mice.[3] Vascular endothelial growth factor levels are elevated in the vitreous fluid from eyes of patients with diabetic retinopathy, and the cytokine is considered a key molecular role player in the neurovascular complications of diabetic retinopathy.[4] Thus, altered selection of mRNAs, such as the one encoding VEGF, for translation represents an intriguing target for novel clinical therapies that move beyond addressing the symptoms of diabetes and attempt to target the underlying molecular mechanisms.

A potential molecular target for preventing hyperglycemia-induced upregulation of VEGF mRNA translation is the translational repressor 4E-BP1. Previous studies have shown that 4E-BP1 expression is elevated in the retina of diabetic mice, and in retinal cells in culture exposed to hyperglycemic conditions.[5] Yet, in the retina of mice lacking 4E-BP1, VEGF expression remains unchanged in response to diabetes.[5] 4E-BP1 regulates the selection of mRNAs for translation through sequestration of the cap-binding protein eIF4E that recognizes the m^7GTP cap structure found at the 5′-terminus of all eukaryotic mRNAs.[6] Variation in availability of eIF4E serves as a critical regulator of gene expression patterns, as some messages, such as the one that encodes VEGF, contain RNA elements that facilitate ribosome recruitment and translation independent of eIF4E and the 5′-cap structure (i.e., cap-independent translation).[7] Diabetes-induced hyperglycemia mediates a 4E-BP1–dependent shift in gene expression that is driven by downregulation of cap-dependent translation concomitant with upregulation of cap-independent translation.[8] Thus, the effects of hyperglycemia on 4E-BP1 not only alter global gene expression patterns during diabetes, but also function as a key modulator of the changes in growth factor expression that are causally linked to development of complications in the retina.[9]

The interaction of 4E-BP1 with eIF4E is negatively regulated by mammalian target of rapamycin (mTORC1)-dependent phosphorylation of serine and threonine residues on 4E-

Investigative Ophthalmology & Visual Science

BP1.[10] In the retina of diabetic rats, the interaction of 4E-BP1 with eIF4E is elevated, and a similar effect is observed in retinal cells in culture upon exposure to hyperglycemic conditions.[3,5] Hyperglycemia-induced sequestration of eIF4E is in part due to attenuated mTORC1 signaling, as 4E-BP1 phosphorylation is reduced in both the retina of diabetic mice and in retinal cells in culture following exposure to hyperglycemic conditions.[3,5] However, 4E-BP1 is also modified posttranslationally by the covalent addition of *O*-linked *N*-acetylglucosamine (*O*-GlcNAc) in a manner that promotes sequestration of eIF4E independent of 4E-BP1 phosphorylation.[11] Thus, hyperglycemia-driven *O*-GlcNAc modification of 4E-BP1 provides a mechanism in addition to phosphorylation to control its function.

In the retina of diabetic rodents, 4E-BP1 protein expression is transiently elevated 4 to 6 weeks after the induction of diabetes.[5] In the present study, we show that mice lacking 4E-BP1/2 were protected from diabetes-induced visual impairment during this early stage of the disease. Thus, we set out to establish the mechanism whereby diabetes promotes expression of 4E-BP1. Elevated 4E-BP1 protein expression in the retina of diabetic rodents occurs in the absence of changes in 4E-BP1 mRNA expression,[5] suggesting that a posttranscriptional control mechanism regulates its expression. Furthermore, 4E-BP1 mRNA has a relatively short 5′untranslated region (UTR) that appears to lack significant secondary structure or regulatory sequences necessary for translational regulation. We report that both hyperglycemic conditions and enhanced global *O*-GlcNAcylation are associated with attenuation of 4E-BP1 degradation. This finding supports previous reports that *O*-GlcNAcylation serves as a global mechanism for protecting proteins against proteasomal degradation.[12–15] In the present study, we identified a conserved PEST motif in the C-terminus of 4E-BP1, which includes Thr82, a residue critical for 4E-BP1 *O*-GlcNAcylation.[11] In many cases, phosphorylation of Ser or Thr residues within a PEST motif results in accelerated protein instability.[16] Thus, many PEST motifs are not recognized by the ubiquitin ligase system until they are tagged for degradation by phosphorylation. However, *O*-GlcNAc moieties, which can competitively occupy the same Ser or Thr residues that are targeted by phosphorylation, potentially block the phosphorylation events that target proteins for degradation. To evaluate the role of this motif in reduced 4E-BP1 turnover, we performed alanine substitution on residues within the PEST domain and found that these sites regulated 4E-BP1 polyubiquitination and interaction with the E3 ligase complex KLHL25-CUL3. Overall, the findings support a model whereby elevated 4E-BP1 expression in the retina of diabetic mice is the result of PEST motif *O*-GlcNAcylation.

Materials and Methods

Materials

Preparation of the 4E-BP1 and eIF4E antibodies has been previously described.[17,18] 4E-BP1 phosphospecific antibodies were purchased from Cell Signaling Technology (Danvers, MA, USA). Goat anti-mouse and goat anti-rabbit IgG horseradish peroxidase–conjugated antibodies were purchased from Bethyl Laboratories (Montgomery, TX, USA). Anti-GAPDH (glyceraldehyde 3-phosphate dehydrogenase) antibody was purchased from Santa Cruz (Dallas, TX, USA), and all other antibodies were purchased from Cell Signaling Technology.

Animals

At ~4 weeks of age, male 4E-BP1/2 double knockout C57BL/6J mice received injections of 50 mg/kg streptozotocin (STZ) dissolved in sodium citrate buffer (pH 4.5) for 5 consecutive days to induce diabetes. Non-littermate wild-type mice were treated similarly as controls. Alternatively, male Sprague-Dawley rats (Charles River, Wilmington, MA, USA) weighing ~200 g received a single intraperitoneal injection containing 65 mg/kg STZ. Control rodents received an equivalent volume of sodium citrate buffer. Diabetic phenotype was confirmed by blood glucose concentrations > 250 mg/dL in freely fed animals. Glycemic control was achieved in diabetic mice by twice-daily subcutaneous injections of phlorizin (200 mg/kg) during the last 7 full days of the experiment, as well as 3 hours prior to tissue harvest. Where indicated, mice received 50 mg/kg Thiamet G (TMG) or phosphate buffer as a control via intraperitoneal injection. Retinas were harvested 4 weeks after STZ or 24 hours after TMG injections, flash-frozen in liquid nitrogen, and later sonicated in 250 µL extraction buffer as previously described.[3] The homogenate was centrifuged at 10,000*g* for 5 minutes at 4°C, and the supernatant was prepared for analysis as described below. All experimental procedures adhered to the ARVO Statement for the Use of Animals in Ophthalmic and Vision Research and were approved by the Pennsylvania State College of Medicine Institutional Animal Care and Use Committee.

Behavioral Assessment of Visual Thresholds

A virtual optomotor system (Optomotry; Cerebral Mechanics, White Plains, NY, USA) was used to assess visual function in control and diabetic mice as previously described.[19] Briefly, four inward-facing liquid crystal display monitors were used to create the illusion of a virtual cylinder rotating around a mouse. Contrast sensitivity (CS) and spatial frequency thresholds (SF) were assessed using a video camera to monitor elicitation of the optokinetic reflex. Contrast sensitivity was assessed at a SF of 0.092 cyc/deg. Spatial frequency was assessed at 100% contrast. The CS and SF thresholds were identified as the highest values that elicited the reflexive head movement. Both thresholds were averaged over three trials on consecutive days.

Cell Culture

TR-MUL retinal Müller cells were provided by K. Hosoya (Toyama Medical and Pharmaceutical University). TR-MUL and HEK293E cell cultures were maintained in Dulbeco's modified Eagle's medium (DMEM) lacking sodium pyruvate and contained 5 mM glucose (Gibco, Carlsbad, CA, USA) supplemented with 10% fetal bovine serum (Atlas Biologicals, Fort Collins, CO, USA) and 1% penicillin/streptomycin (Gibco). Where indicated, cells were exposed to medium containing 25 to 30 mM glucose or 5 mM glucose supplemented with 20 to 25 mM mannitol to serve as an osmotic control. Transfections were performed using Lipofectamine 2000 (Life Technologies, Carlsbad, CA, USA) according to the manufacturer's instructions. 4E-BP1 tagged with HA was exogenously expressed in cells using the pCMV6-4E-BP1-HA plasmid. This construct was generated by adding a C-terminal HA tag to the pCMV6-4E-BP1 plasmid (purchased from Origene Technologies, Rockville, MD, USA), using the forward 5′-AATGCTCGAGTCAAGCG TAATCTGGAACATCGTATGGGTAAATGTCCATCTCAAATTGT GA-3′ and reverse 5′-TCCGGAATTCCCGGGATAT-3′ primers and cloning the resulting PCR product back into pCMV6 using *Eco*RI and *Xho*I. Site-directed mutagenesis to generate 4E-BP1-T82A was previously described.[11] Additional 4E-BP1 variants were generated using Quick-Change Lightning (Agilent Technologies, Wilmington, DE, USA) and the primers listed in Supplementary Table S1. Where indicated, cells were treated with 1 µM cycloheximide (A.G. Scientific, Inc., San Diego, CA, USA), 50 nM TMG, 10 nM ST045849

(TimTec, Inc., Newark, DE, USA), 5 μM CHIR99021 (Tocris Bioscience, Anonmouth, Bristol, UK) 10 nM TORIN2 (Tocris Bioscience), and/or 10 μM MG-132 (Calbiochem, San Diego, CA, USA). To evaluate 4E-BP1 synthesis and turnover, cells were radiolabeled via the inclusion of 30 μCi/mL L-[^{35}S]methionine (Amersham, Marlborough, MA, USA) into cell culture medium for 1 or 16 hours, respectively. To evaluate the rate of [^{35}S]methionine-labeled 4E-BP1 turnover, isotope-containing medium was replaced with DMEM supplemented with nonradiolabeled 20 mM L-methionine for 24 hours. Cells were harvested in lysis buffer and centrifuged at 10,000*g* for 5 minutes at 4°C and analyzed as described below. For small interfering RNA (siRNA) studies, complementary RNAs were obtained from Cell Signaling Technology to knock down GSK3α/β (glycogen synthase kinase 3) and transfected using Lipofectamine 2000 according to the manufacturer's protocol.

Protein Analysis

A fraction of supernatant was added to SDS sample buffer, boiled for 5 minutes, and analyzed by Western blotting as previously described.[3] Quantitation of total 4E-BP1 protein expression and phosphorylation was performed as previously described.[11]

Immunoprecipitations

Immunoprecipitations were performed by incubating 1000*g* supernatants of retina homogenates or cell culture lysates with monoclonal anti-eIF4E or anti-4E-BP1 antibody as previously described.[8] However, in retinal eIF4E immunoprecipitations, CHAPS lysis buffer [10 mM potassium phosphate (pH 7.2), 0.3% CHAPS, 1 mM EDTA, 5 mM EGTA, 10 mM $MgCl_2$, 50 mM β-glycerophosphate] was substituted for the conventional lysis and wash buffers. To evaluate 4E-BP1 *O*-GlcNAc modification, lysis and wash buffers were supplemented with 1 mM N-Acetyl-D-glucosamine (Sigma-Aldrich Corp., St. Louis, MO, USA) and 10 μM PUGNAc (Tocris Bioscience). For anti-HA and anti-FLAG immunoprecipitations, 10 μL either anti-HA-agarose affinity resin (Sigma-Aldrich Corp.) or EZview Red anti-FLAG M2 affinity gel (Sigma-Aldrich Corp.) was used. Beads were washed with CHAPS lysis buffer and blocked with CHAPS lysis buffer containing 1% BSA prior to use. Cells were harvested in CHAPS lysis buffer supplemented with 1 mM sodium vanadate and 10 μL/ml protease inhibitor mixture and lysed for 30 minutes at 4°C. For evaluation of polyubiquinated isoforms, buffers were supplemented with 5 mM N-ethylmaleimide (Sigma-Aldrich Corp.). Cell supernatants were collected by centrifuging lysates 3 minutes at 1000*g* and then incubated with the affinity resin for 2 hours. The affinity resin was washed (3×) with cold CHAPS lysis buffer or RIPA (radioimmunoprecipitation assay) wash buffer (25mM Tris-HCl pH 7.6, 150 mM NaCl, 1% NP-40, 1% sodium deoxycholate, 0.1% SDS), suspended in SDS sample buffer, and boiled for 5 minutes. The immunoprecipitates were subjected to SDS-PAGE and Western blot analysis. Alternatively, autoradiography was used to evaluate the rate of [^{35}S]methionine-labeled 4E-BP1 turnover.

Statistical Analysis

Data are expressed as mean + SE. Statistical analysis was performed with Prism (GraphPad, Inc., La Jolla, CA, USA). Two-way analysis of variance was used to identify differences among group means. When identified, a Student's *t*-test was used post hoc to compare differences between groups. $P < 0.05$ was considered statistically significant.

Results

Diabetes-Induced Visual Dysfunction Is Delayed in 4E-BP1/2–Deficient Mice

In the present study we directly assessed diabetes-induced visual dysfunction in 4E-BP1/2–deficient mice by measurement of the optokinetic response. Following 6 weeks of STZ-induced diabetes, wild-type mice exhibited a deficit in CS, whereas 4E-BP1/2–deficient mice failed to do so (Fig. 1A). Moreover, SF was attenuated in diabetic wild-type mice as compared to nondiabetic wild-type mice; however, diabetic and nondiabetic 4E-BP1/2–deficient mice exhibited similar SF (Fig. 1B). Notably, both blood glucose concentrations were similar in wild-type and 4E-BP1–deficient mice (Supplementary Fig. S1). The protective effects of 4E-BP1/2 ablation on CS were maintained at least 10 weeks after STZ administration (Fig. 1C); however, both wild-type and 4E-BP1/2–deficient mice exhibited reduced SF at this time point (Fig. 1D). Moreover, both CS and SF thresholds were reduced in wild-type and 4E-BP1/2–deficient mice 14 weeks after STZ administration (Fig. 1E).

Hyperglycemia Produces an Elevation in 4E-BP1 Expression and *O*-GlcNAcylation in the Retina

We previously demonstrated that 4E-BP1 protein expression is elevated in the retina of rodents as early as 4 weeks after the onset of diabetes and returns to basal levels by 12 weeks.[5] To assess the role of hyperglycemia in elevated 4E-BP1 expression, diabetic mice were administered phlorizin to lower blood glucose concentrations by blocking intestinal glucose absorption and producing renal glucosuria.[20] As previously observed,[8] twice-daily administration of phlorizin reduced serum glucose concentrations in diabetic mice (Fig. 2A). Following 4 weeks of STZ-induced diabetes, total retinal 4E-BP1 expression was elevated in diabetic mice as compared to nondiabetic cohorts (Fig. 2B). Notably, phlorizin reduced 4E-BP1 expression in the retina of diabetic mice (Fig. 2B). Similarly, 4E-BP1 expression was modestly elevated in the retina of a previously described[3] cohort of diabetic rats, whereas phlorizin-induced glycemic control reduced its expression to a value not significantly different from that in nondiabetic rats (Fig. 2C). To determine if elevated 4E-BP1 expression was associated with *O*-GlcNAcylation of the protein, 4E-BP1 was immunoprecipitated from retinas. Indeed, STZ-induced diabetes elevated *O*-GlcNAcylation of 4E-BP1 in the retina, whereas upon phlorizin treatment, levels of the covalent modification were not different from that in nondiabetic controls (Fig. 2D). To evaluate if *O*-GlcNAcylation alters retinal 4E-BP1 expression, mice were treated with TMG, which inhibits *O*-GlcNAcase (OGA), the enzyme that catalyzes the removal of *O*-GlcNAc residues from proteins. Thiamet G enhanced global protein *O*-GlcNAcylation (Fig. 2E), and produced an elevation in 4E-BP1 expression (Fig. 2F) concomitant with reduced phosphorylation of 4E-BP1 (Fig. 2G) in the retina.

O-GlcNAcylation Facilitates Hyperglycemia-Induced 4E-BP1 Expression

To further evaluate the mechanism whereby hyperglycemic conditions elevated 4E-BP1 expression, we employed rat Müller (TR-MUL) cells in culture exposed to medium containing either control (5 mM) or high (30 mM) concentrations of glucose. Müller cells are the main glial cells of the retina and a likely target of the pathologic effects of hyperglycemia.[21,22] Moreover, diabetes-induced Müller cell abnormalities occur in temporal accord with the onset of visual deficiencies observed

Investigative Ophthalmology & Visual Science

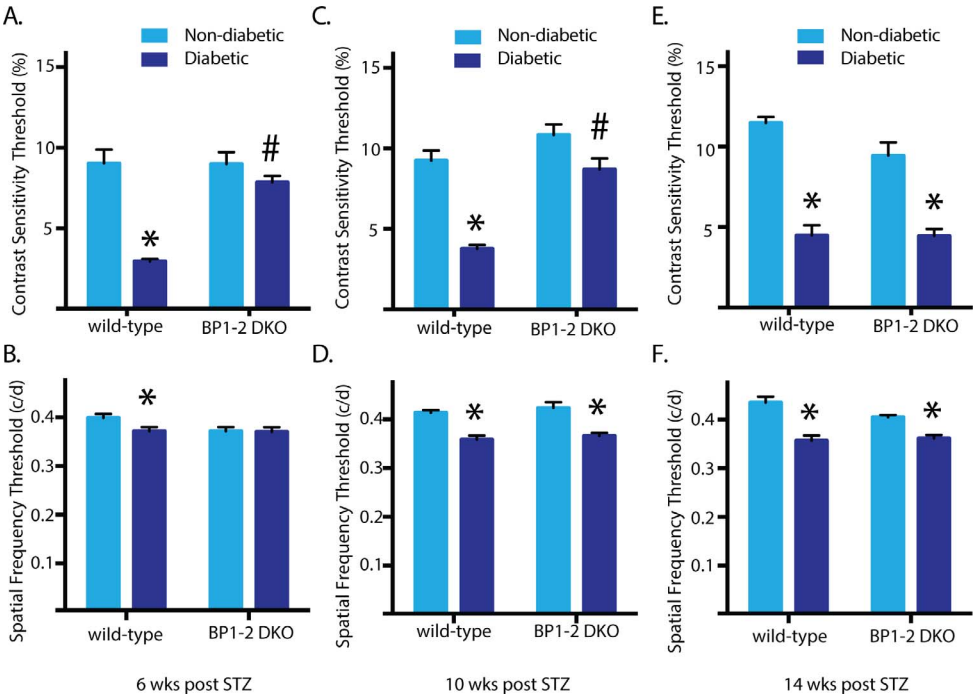

Figure 1. Diabetes-induced visual dysfunction is delayed in 4E-BP1/2–deficient mice. Visual function was assessed by optomotry optokinetic testing after 6 (**A**, **B**), 10 (**C**, **D**), and 14 weeks (**E**, **F**) of diabetes. Contrast sensitivity (**A**, **C**, **E**) and spatial frequency thresholds (**B**, **D**, **F**) were obtained in nondiabetic and diabetic wild-type and 4E-BP1/2 double knockout (BP1/2-DKO) mice. Contrast sensitivity threshold is expressed as the reciprocal value of the contrast sensitivity score. Values are means + SE ($n = 4$–7). Statistically significant differences ($P < 0.05$) are denoted * versus control and # versus wild type.

here.[23] Following exposure to medium containing 30 mM glucose, 4E-BP1 expression and global *O*-GlcNAcylation levels were elevated in TR-MUL cells as compared to cells exposed to control medium containing 5 mM glucose (Fig. 3A). This observation supports a previous report[5] showing that a similar effect of hyperglycemic conditions on 4E-BP1 expression was observed in TR-MUL cells in culture. To extend these observations, we evaluated the role of global *O*-GlcNAcylation on 4E-BP1 expression. When TR-MUL cells were exposed to medium containing TMG, both global protein *O*-GlcNAcylation and 4E-BP1 expression were elevated (Fig. 3B). To determine the necessity of *O*-GlcNAcylation in the effect of hyperglycemic conditions, TR-MUL cells were exposed to medium containing 30 mM glucose concentrations in combination with ST045849. ST045849 inhibits *O*-GlcNAc Transferase (OGT), the enzyme that catalyzes the addition of *O*-GlcNAc residues to the hydroxyl side chains of proteins. In the presence of ST045849, hyperglycemic conditions failed to produce an elevation in global *O*-GlcNAcylation levels or 4E-BP1 expression (Fig. 3C).

Hyperglycemic Conditions and Thiamet G Elevate 4E-BP1 Expression via a Reduction in its Rate of Degradation

To investigate the mechanism responsible for elevated expression of 4E-BP1, its rate of synthesis was assessed by incorporation of [^{35}S]methionine into the protein in cells incubated under hyperglycemic or control conditions. There was no significant difference in incorporation of [^{35}S]methionine into 4E-BP1 (Fig. 4A), suggesting that elevated expression of 4E-BP1 was not the result of enhanced synthesis. To evaluate the rate of 4E-BP1 degradation, cells were incubated in the presence of cycloheximide to inhibit protein synthesis. While the rate of 4E-BP1 turnover was relatively slow under hyperglycemic conditions, under control conditions the protein was almost completely degraded following prolonged exposure to cycloheximide (Fig. 4B). Together these findings suggest that the elevated expression of 4E-BP1 that is observed following exposure to hyperglycemic conditions is the result of attenuated degradation of the protein. To evaluate the effect of *O*-GlcNAcylation on the rate of 4E-BP1 degradation, cells were exposed to TMG to elevate global protein *O*-GlcNAcylation (Fig. 4C) and then cycloheximide was administered. In the presence of medium containing TMG, 4E-BP1 exhibited a reduced rate of degradation (Fig. 4D). To provide further support that *O*-GlcNAcylation reduces 4E-BP1 turnover, cells were labeled with [^{35}S]methionine in the presence or absence of TMG. The [^{35}S]methionine-containing medium was then replaced with medium containing an excess of nonradiolabeled methionine in the presence or absence of TMG, and 4E-BP1 was immunoprecipitated after 0 or 24 hours. In support of our finding with cycloheximide, the level of [^{35}S]methionine-labeled 4E-BP1 was reduced in vehicle-treated cells after 24 hours, whereas the level of [^{35}S]methionine-labeled 4E-BP1 was maintained in cells treated with TMG (Fig. 4E).

Identification of a PEST Motif in the C-Terminus of 4E-BP1

Unlike 4E-BP1, the 4E-BP2 isoform does not exhibit enhanced binding to eIF4E in the retina of diabetic rodents.[5] Thus, we evaluated the effect of hyperglycemic conditions on 4E-BP2 expression and turnover. 4E-BP2 did not exhibit elevated expression or a differential rate of turnover upon exposure to hyperglycemic conditions (Fig. 5A). The amino acid sequences of 4E-BP1 and 4E-BP2 were then compared in silico using the Web-based algorithm epestfind (EMBOSS explorer, http://emboss.bioinformatics.nl/cgi-bin/emboss/epestfind [in the public domain]). This algorithm searches for PEST motifs

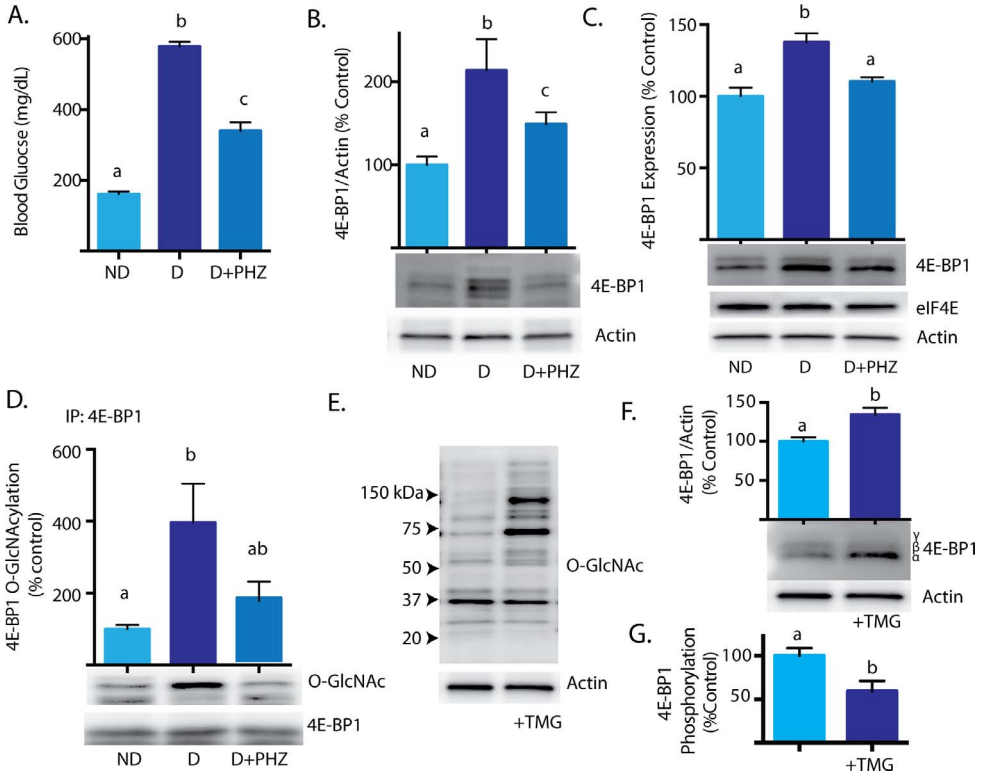

Figure 2. Diabetes-induced hyperglycemia or the *O*-GlcNAcase inhibitor Thiamet G produces an elevation in 4E-BP1 expression in the retina. Diabetes was induced in mice (**A**, **B**) or rats (**C**, **D**) by STZ injection. Four weeks after the induction of diabetes, phlorizin (PHZ) was administered twice daily for 7 days to lower blood glucose concentrations. (**B**, **C**) Retina supernatant fractions were prepared and 4E-BP1 content was measured by Western blot analysis. Retina supernatant fractions were prepared and the content of 4E-BP1 was assessed by Western blot. (**D**) 4E-BP1 was immunoprecipitated (IP) from retina supernatant fractions and subjected to Western blot analysis to assess *O*-GlcNAcylation of the protein. Blood glucose concentrations and 4E-BP1 phosphorylation for rats were previously reported.[3] (**E–G**) Global protein *O*-GlcNAcylation was enhanced in the retina by intraperitoneal injection of the *O*-GlcNAcase inhibitor, Thiamet G (TMG, 50 mg/kg). Global protein *O*-GlcNAcylation (**E**), 4E-BP1 content (**F**), and 4E-BP1 phosphorylation (**G**) were evaluated by Western blot. Values are means + SE ($n = 8$ [**A–D**] and 4 [**F–G**]). Statistically significant differences ($P < 0.05$) are denoted by the presence of different letters *above the bars* on the graphs.

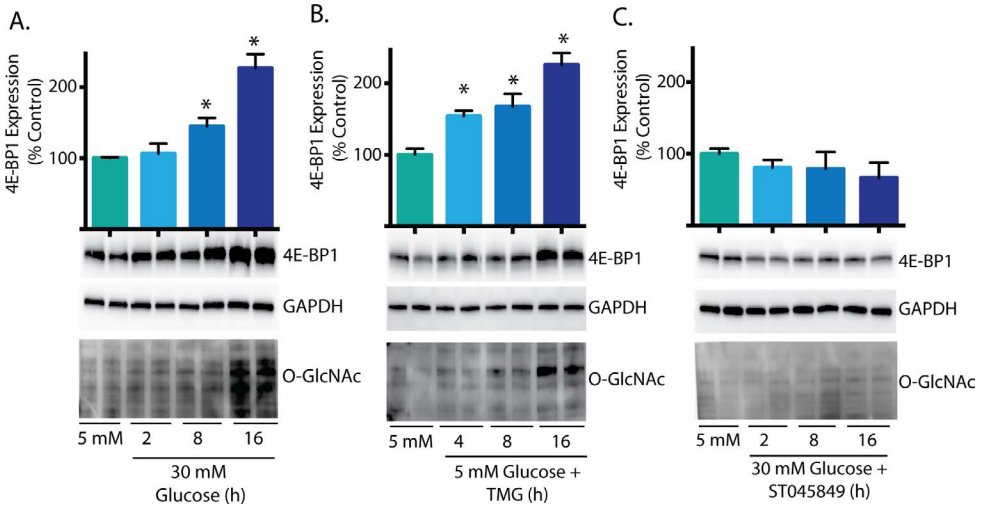

Figure 3. *O*-GlcNAcylation produces an elevation in 4E-BP1 expression. Rat TR-MUL Müller cell cultures were maintained in DMEM containing 5 mM glucose and supplemented with 10% heat-inactivated FBS. (**A**) Cells were exposed to medium containing 30 mM glucose. (**B**) Cells were exposed to the *O*-GlcNAcase inhibitor Thiamet G (TMG) to inhibit *O*-GlcNAc cycling and elevate global *O*-GlcNAcylation levels. (**C**) Cells were exposed to medium containing 30 mM glucose in the presence of the *O*-GlcNAc Transferase inhibitor ST045849 (10 nM) to prevent hyperglycemia-induced protein *O*-GlcNAcylation. 4E-BP1 content as well as global *O*-GlcNAcylation was assessed in cell lysates by Western blot analysis relative to GAPDH. Values are means + SE ($n = 4$). Statistically significant differences are denoted * versus control, $P < 0.05$.

Investigative Ophthalmology & Visual Science

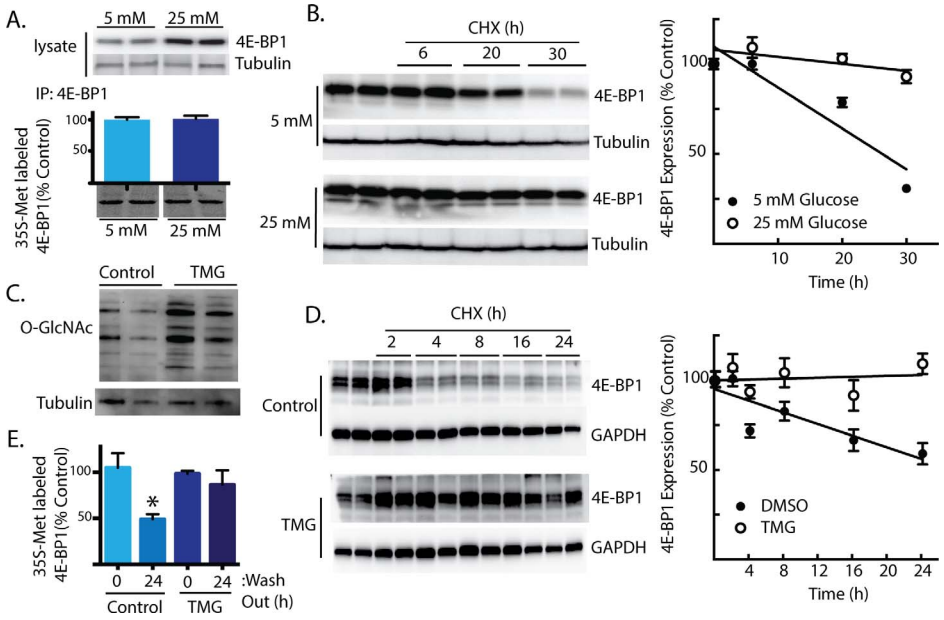

Figure 4. 4E-BP1 expression is elevated via a reduction in its rate of degradation under hyperglycemic conditions and following exposure to Thiamet G. HEK293E cells were maintained in DMEM containing 5 mM glucose and supplemented with 10% heat-inactivated FBS. 4E-BP1 content relative to tubulin was measured by Western blot analysis. (**A**) HEK293E cells were incubated in medium containing [^{35}S]methionine and either 25 mM glucose or 5 mM glucose supplemented with 20 mM mannitol as an osmotic control for 1 hour. 4E-BP1 was immunoprecipitated and subjected to SDS-PAGE. The gel was dried and [^{35}S] incorporation was detected upon exposure to film to evaluate the rate 4E-BP1 synthesis. (**B**) HEK293E cells were exposed to medium containing either 25 mM glucose or 5 mM glucose supplemented with 20 mM mannitol for 16 hours. Cells were treated with 1 mM cycloheximinde (CHX) and harvested at 3, 6, 24, and 30 hours post treatment. (**C**) HEK293E cells were exposed to Thiamet G (TMG) for 4 hours to increase global protein *O*-GlcNAcylation. (**D**) HEK293E cells were exposed to medium containing Thiamet G for 4 hours, then treated with 1 mM cycloheximide (CHX) and harvested at 2, 4, 8, 16, and 30 hours post treatment. 4E-BP1 content relative to GAPDH was measured by Western blot analysis. (**E**) HEK293E cells were incubated in medium containing [^{35}S]methionine in the presence or absence of TMG for 16 hours. Isotope-containing medium was washed out with DMEM supplemented with 20 mM L-methionine for 0 or 24 hours. 4E-BP1 was immunoprecipitated and subjected to autoradiography to evaluate turnover of the isotope-labeled protein. Values are mean + SE ($n = 4$). Statistically significant differences are denoted * versus control, $P < 0.05$.

characterized by hydrophilic stretches of amino acids with high concentrations of acidic and hydroxylated amino acids and the strict absence of positively charged amino acids. PEST motifs have long been associated with targeting proteins for degradation through the ubiquitin–proteasome pathway.[24] Valid PEST motifs above a threshold score of 5.0 are of particular interest. A single strong PEST motif (+11.69) was assigned to the highly conserved residues 79 to 90 of 4E-BP1 (Fig. 5B). Notably, only poor PEST motifs were identified in 4E-BP2 (−1.30 to −21.42), and the corresponding residues that were aligned with the PEST motif in 4E-BP1 were poorly conserved (Fig. 5C).

Identification of a Consensus GSK3 Site Within the PEST Motif

Since *O*-GlcNAcylation of 4E-BP1 at Thr82[11] potentially blocks activation of the PEST motif by a competing phosphorylation event, we evaluated the amino acid sequence around this residue to determine if it was a consensus phosphorylation site for any known kinases. Analysis of the sequences surrounding Thr82 in silico using Scansite (http://scansite.mit.edu [in the public domain]) identified Thr82 as a consensus GSK3 phosphorylation site. GSK3 phosphorylation-dependent proteolysis has been proposed as a global mediator of protein turnover.[25] GSK3 is well known for its role in marking β-catenin for ubiquitination and proteolysis,[26,27] but a similar effect has been reported for dozens of other proteins.[25] To evaluate GSK3 as a regulator of 4E-BP1 stability, cells were exposed to the GSK3 inhibitor CHIR99021. CHIR99021 elevated 4E-BP1 expression in a dose-dependent manner (Fig. 5D), such that there was a 2-fold increase after 16 hours (Fig. 5E). Similarly, 4E-BP1 expression was elevated when siRNAs directed against GSK3α/β mRNA were used to knock down GSK3 subunit expression (Fig. 5F).

Thr82/Ser86 Regulate Ubiquitination and Degradation of 4E-BP1

The best-explored GSK3 substrates require priming phosphorylation at a residue located 4 amino acids C-terminally to the GSK3 target residue.[28] Accordingly, GSK3-mediated phosphorylation of Thr82 potentially requires priming phosphorylation at Ser86. To evaluate a potential role for Thr82 and Ser86 in 4E-BP1 polyubiquitination, we coexpressed HA-tagged 4E-BP1 T82A, S86A, and the double alanine mutant T82A/S86A (AA) with FLAG-tagged ubiquitin; HA-tagged 4E-BP1 T82A, S86A, and AA all exhibited reduced polyubiquitination as compared to wild-type 4E-BP1 (Fig. 5G). Thus, disruption of the PEST motif via alanine substitution at Thr82 or Ser86 was sufficient to inhibit polyubiquitination of 4E-BP1. As observed with endogenous 4E-BP1, the rate of HA-tagged wild-type 4E-BP1 turnover was reduced under hyperglycemic as compared to control conditions (Fig. 5H). However, as compared to wild type, the 4E-BP1 T82A variant exhibited enhanced stability in response to either hyperglycemic or control conditions (Fig. 5I). Notably, the rate of 4E-BP1 T82A turnover was not different under hyperglycemic as compared to control conditions. Importantly, 4E-BP1 T82A stability was similar to that observed when all four lysines (Lys57, Lys69, Lys73, Lys105) were mutated to arginine to prevent polyubiquitination (Fig. 5J).

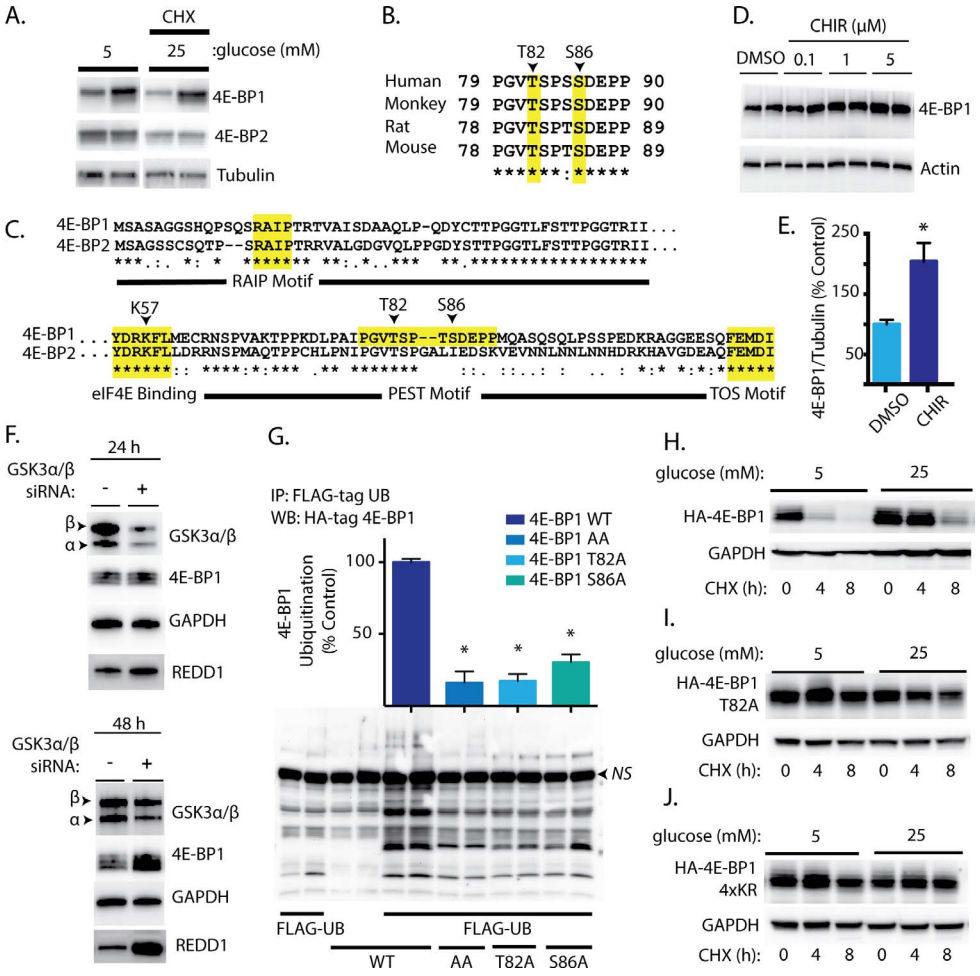

Figure 5. Identification of a C-terminal PEST motif that regulates 4E-BP1 polyubiquitination and turnover. (**A**) HEK293E cells were maintained in DMEM containing 5 mM glucose and supplemented with 10% heat-inactivated FBS. Cells were exposed to medium containing either 25 mM glucose or 5 mM glucose supplemented with 20 mM mannitol in the presence of 1 mM cycloheximide (CHX) or vehicle for 24 hours. 4E-BP1 and 4E-BP2 protein content was assessed relative to tubulin by Western blot analysis. (**B**) Alignment of amino acid sequences of the 4E-BP1 PEST motif. (**C**) Alignment of 4E-BP1 and 4E-BP2 amino acid sequences. (**D**) TR-MUL cells were maintained as described above and treated with the GSK3 inhibitor CHIR99021 (CHIR) for 16 hours as indicated. (**E**) TR-MUL cells were maintained in medium in the presence or absence of CHIR, and 4E-BP1 protein content relative to tubulin was assessed by Western blot analysis. Values are means + SE ($n = 4$). Statistically significant differences are denoted * versus control, $P < 0.05$. (**F**) HEK293E cells were transfected with siRNA directed against GSK3α/β for 24 or 48 hours. GSK3α/β, 4E-BP1, and actin protein content was assessed by Western blot analysis. (**G–J**) HEK293E cells were transiently transfected with plasmids encoding FLAG-tagged ubiquitin (FLAG-UB), wild-type C-terminally HA-tagged 4E-BP1 (HA-4E-BP1), T82A, S86A, T28A/S86A (AA), or K57R/K69R/K73R/K105R (4×KR) as indicated. (**G**) HEK293E cells were exposed to TORIN2 for 16 hours and MG132 for 4 hours. The mTOR active site inhibitor TORIN2 was used to promote the presence of high molecular weight 4E-BP1 isoforms, as previously described.[29] FLAG-tag immunoprecipitates were prepared and subjected to Western blot analysis using anti-HA-tag antibody. High molecular weight HA-tagged 4E-BP1 isoforms were quantitated. NS, nonspecific band. (**H–J**) HEK293E cells were grown in media containing either 25 mM glucose or 5 mM glucose supplemented with 20 mM mannitol. Cells were treated with 1 mM cycloheximide (CHX) as indicated. 4E-BP1 content relative to GAPDH was assessed by Western blot analysis.

PEST Motif Regulates 4E-BP1 Interaction With the KLHL25-CUL3 Complex

A cullin-RING-based BCR (BTB-CUL3-RBX1) E3 ubiquitin-protein ligase complex has been previously implicated in the polyubiquitination of 4E-BP1 and its subsequent proteasomal degradation.[29] The BTB domain-containing protein KLHL25 functions as a substrate-specific adaptor within this complex by binding to 4E-BP1. The scaffolding protein CUL3 links KLHL25 with the RING finger protein.[30] Unlike eIF4E, which coimmunoprecipitated with both N-terminally and C-terminally HA-tagged 4E-BP1, CUL3 coimmunoprecipitated only with C-terminally tagged 4E-BP1 (Fig. 6A). Thus, the presence of a tag at the N-terminus of the protein interferes with its association with CUL3, and for subsequent studies C-terminally HA-tagged 4E-BP1 was used. Coimmunoprecipitation of eIF4E with C-terminally HA-tagged 4E-BP1 T82A/S86A was reduced as compared to that of wild-type 4E-BP1 (Fig. 6B). A similar reduction in the interaction with eIF4E was observed with both 4E-BP1 T82A and S86A (Fig. 6C). Surprisingly, coimmunoprecipitation of CUL3 with HA-tagged 4E-BP1 T82A/S86A was increased as compared to wild-type 4E-BP1 (Figs. 6B, 6D), despite reduced polyubiquitination of this variant (Fig. 5G). Again, a similar effect was observed with T82A and S86A variants (Fig. 6D). Thus, integrity of the PEST domain was not necessary for interaction with the KLHL25-CUL3 E3 ubiquitin ligase complex. One possible explanation is that reduced eIF4E interaction permits increased association with KLHL25-CUL3. However, both 4E-BP1 and CUL3 coimmunoprecipitated with eIF4E, suggesting that the interactions of CUL3 and eIF4E are not mutually exclusive (Fig. 6E). A previous report supports that the KLHL25-CUL3 complex does not bind to 4E-BP1 at the

Investigative Ophthalmology & Visual Science

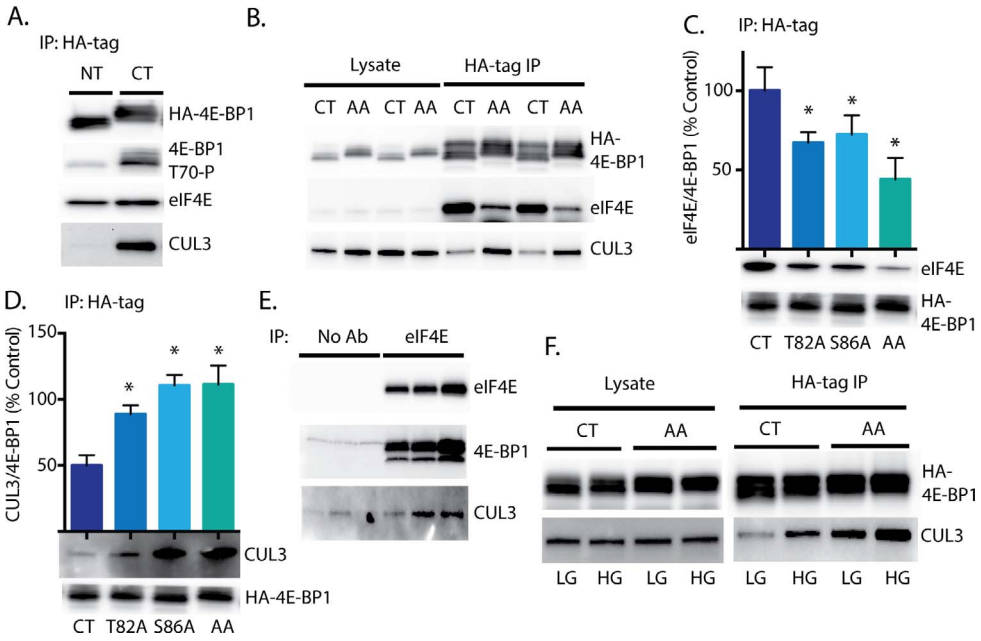

Figure 6. PEST motif in C-terminus of 4E-BP1 regulates coimmunoprecipitation with the E3 ligase CUL3. HEK293E cells were maintained in DMEM containing 5 mM glucose and supplemented with 10% heat-inactivated FBS. (**A–D**, **F**) HEK293E cells were transiently transfected with plasmids encoding wild-type N-terminally HA-tagged 4E-BP1 (NT), wild-type C-terminally HA-tagged 4E-BP1 (CT), T82A, S86A, or T82A/S86A (AA) as indicated. (**B–D**, **F**) HEK293E cells were exposed to TORIN2 for 16 hours and MG132 for 4 hours. HA-tag immunoprecipitates were prepared and subjected to Western blot analysis. Values are means + SE ($n = 3$). Statistically significant differences are denoted * versus wild-type plasmid, $P < 0.05$. (**E**) eIF4E was immunoprecipitated (IP) from retina supernatant fractions and subjected to Western blot analysis to assess the coimmunoprecipitation of 4E-BP1 and CUL3 relative to no-antibody controls (No Ab). (**F**) HEK293E cells were exposed to medium containing either 5 mM glucose supplemented with 20 mM mannitol (LG) or 30 mM glucose supplemented with Thiamet G (HG).

same site as eIF4E.[29] In support of the report, coimmunoprecipitation of eIF4E with N-terminally HA-tagged 4E-BP1 was not elevated as compared to C-terminally tagged 4E-BP1 (Fig. 6A). Overall, these findings support that the 4E-BP1 interaction with CUL3 is independent of eIF4E binding. To evaluate the effect of hyperglycemia on CUL3 binding, cells were exposed to hyperglycemic conditions prior to immunoprecipitation. Exposure to hyperglycemic conditions increased the coimmunoprecipitation of CUL3 with wild-type 4E-BP1 to a level similar to that observed with the T82A/S86A variant (Fig. 6F). Overall, the data support a model where modification of the PEST motif via 4E-BP1 *O*-GlcNAcylation or alanine substitution at Thr82/Ser86 promotes CUL3 retention by blocking polyubiquitination and release of the E3 ubiquitin ligase complex (Supplementary Fig. S2).

Discussion

The failure of key regulatory proteins to be expressed appropriately leads to an array of human pathologies. The findings of the present study provide new insight into the mechanism whereby diabetes-induced hyperglycemia enhances expression of the translational repressor 4E-BP1 in the retina. While elevated 4E-BP1 expression has been previously linked to hyperglycemia-mediated VEGF expression in the retina of diabetic rodents,[5] we demonstrated here that 4E-BP1/2 ablation protects against early visual dysfunction in diabetic mice. Moreover, we demonstrated that elevated 4E-BP1 expression was mediated by hyperglycemia per se, as phlorizin administration to normalize blood glucose levels prevented the effect. This observation is supported by previous studies utilizing retinal Müller cells in culture, where hyperglycemic conditions enhanced 4E-BP1 abundance.[5] Retinal Müller cells are a likely target of the pathologic effects of hyperglycemia, as they are the only cell type in the retina to express GLUT2 glucose transporters,[31] which exhibit a high capacity (but low affinity) for glucose. In cells lacking GLUT2, glucose uptake is quickly saturated under hyperglycemic conditions; however, GLUT2-mediated glucose transport will continue to rise under such conditions. Herein we extended the previous studies by demonstrating that *O*-GlcNAcylation elevated 4E-BP1 expression in the retina.

Since its discovery in the 1980s,[32] protein *O*-GlcNAcylation has emerged as a critical mediator in a range of cellular functions,[33–35] including protein translation.[15] The addition of *O*-GlcNAc (*O*-GlcNAcylation) to the hydroxyl side chain of serine or threonine residues is driven by glucose flux through the hexosamine biosynthetic pathway, which converts the sugar to UDP-N-acetylglucosamine (UDP-GlcNAc), the donor substrate for addition of N-acetyl glucosamine.[32] The *O*-GlcNAcylation cycling enzymes OGT and OGA both strongly associate with ribosomes,[36] suggesting an important role in regulating mRNA translation. Although only a small percentage of glucose enters the hexosamine biosynthetic pathway under normal physiological conditions, diabetes and hyperglycemic conditions dramatically elevate flux through the pathway and promote production of UDP-GlcNAc.[37]

Protein *O*-GlcNAcylation and phosphorylation site-specifically modify hydroxyl side chains of serine/threonine residues in a competitive manner that allows for extensive crosstalk.[38] While there is not a strict consensus sequence for *O*-GlcNAc modification, most sites occur in a serine/threonine-enriched region near a proline and valine residue (i.e., PVS/T).[34] Thus, it is not surprising that many known *O*-GlcNAcylation sites are coregulated by proline-directed kinases, such as GSK3.[39] In the present study, alanine substitution to disrupt a consensus GSK3 phosphorylation site in 4E-BP1 at Thr82 was sufficient to prevent polyubiquitination and degradation of the protein.

Phosphorylation of 4E-BP1 on Thr82[40–42] and Ser86[43–45] has been previously detected in large-scale phosphoproteomic studies. Moreover, GSK3β was recently shown to phosphorylate 4E-BP1.[46] Intriguingly, a number of kinases that inactivate GSK3,[47–50] including PKC, are activated by hyperglycemia in the retina.[51]

In the present study, we observed a small but significant increase in 4E-BP1 expression in the retina of diabetic as compared to control rodents. It is important to consider that this moderate elevation in 4E-BP1 expression (less than 2-fold) is potentially key to the shift in mRNA translation that occurs in response to hyperglycemic conditions. A similar moderate increase in 4E-BP1 expression mediates a shift from cap-dependent to cap-independent mRNA translation in breast cancer tumors.[52] However, at much higher expression levels, 4E-BP1 is inhibitory to cell growth and proapoptotic.[53] Thus, moderately elevated 4E-BP1 expression in retinal cells is likely critical in promoting the shift in mRNA translation that facilitates hyperglycemia-induced VEGF expression.

4E-BP1 was initially reported to undergo proteasome-mediated degradation in a manner that could be suppressed with either the mTOR inhibitor rapamycin or the proteasome inhibitor MG132.[54] Similarly, hyperphosphorylation of 4E-BP1 in response to phosphatase inhibition also promotes polyubiquitination and degradation of the protein.[55] Conversely, exposure of cells to DNA damage or ionizing radiation results in dephosphorylation of 4E-BP1 and an increase in its stability.[56,57] Together these findings support a model in which phosphorylation of 4E-BP1 promotes its degradation by the proteasome. However, more recently Yanagiya et al.[29] provide evidence for a model in which subpopulations of hypophosphorylated non-eIF4E–bound 4E-BP1 are degraded by the proteasome following KLHL25-CUL3–dependent polyubiquitination. In their model, eIF4E binding to hypophosphorylated 4E-BP1 at the central α-helical $Y(X)_4L\Phi$ motif (X, variable amino acids; Φ, hydrophobic amino acids) obstructs polyubiquitination at Lys57. In the absence of eIF4E, 4E-BP1 can be polyubiquitinated by the KLHL25-CUL3 complex; however, hyperphosphorylated 4E-BP1 is resistant to the effect.[29] In support of this model,[29] the results here demonstrate that eIF4E–bound 4E-BP1 also interacts with dormant KLHL25-CUL3 E3 ligase complex in the presence of eIF4E. The 4E-BP1 T82A/S86A variant exhibited reduced eIF4E binding as compared to wild-type 4E-BP1, yet polyubiquitination and degradation of this protein was attenuated as compared to wild-type 4E-BP1. Thus, in addition to the phosphorylation events that regulate eIF4E binding, other regulatory mechanisms must exist for modulating the stability of 4E-BP1.

Herein, we extend the previous studies by exploring how crosstalk between 4E-BP1 phosphorylation and *O*-GlcNAcylation regulates its stability in response to diabetes-induced hyperglycemia. The findings support a model wherein hyperglycemia-induced *O*-GlcNAcylation represses Lys57 ubiquitination by KLHL25-CUL3 (Supplementary Fig. S2). One potential mechanism whereby *O*-GlcNAcylation of 4E-BP1 blocks ubiquitination is by preventing accelerated protein instability via PEST motif phosphorylation. Importantly, of the 13 phosphorylation sites observed on 4E-BP1, only some are responsible for modulating eIF4E binding and electrophoretic mobility. Thus, if phosphorylation events distinct from those that regulate eIF4E binding promote 4E-BP1 turnover, the model of Yanagiya et al.[29] could be resolved with the previous reports[54–57] suggesting that 4E-BP1 phosphorylation promotes its polyubiquitination and degradation. Of the previously characterized phosphorylation sites, Ser83 is of particular interest with regard to the present study, since it is located within the PEST motif. Phosphorylation of 4E-BP1 at Ser83 is rapamycin insensitive, is unresponsive to either insulin or amino acids, and does not appear to influence eIF4E binding.[58] Importantly, the stoichiometry of 4E-BP1 phosphorylation at Ser83 is notably lower than that of other phosphorylation sites,[58] consistent with the idea that the modification may lead to a less stable isoform. Thus, it is tempting to speculate that 4E-BP1 phosphorylation at Ser83 serves to promote recognition of the motif and binding by the KLHL25-CUL3 E3 ligase complex. In this scenario, hyperglycemia-induced *O*-GlcNAcylation at Thr82 would serve as a checkpoint prior to targeting 4E-BP1 for degradation via polyubiquitination.

The results presented herein establish the role of residues within a C-terminal PEST motif in regulating 4E-BP1 expression. In the retina of diabetic rodents, both 4E-BP1 expression and its sequestration of the cap-binding protein eIF4E are elevated.[5] Remarkably, 4E-BP1/2–deficient mice were protected from early diabetes-induced visual dysfunction. Thus, attenuation of 4E-BP1 degradation potentially drives the pathologic expression of genes linked to the development of diabetic retinopathy. Notably, early vision protection in diabetic 4E-BP1/2–deficient mice was later followed by manifestation of visual dysfunction similar to that of wild-type mice. Thus, 4E-BP1/2 ablation protects from early events that contribute to visual dysfunction, yet other mechanism(s) (e.g., transcriptional changes in VEGF expression) must contribute to later stages of this disease. Whereas, SF was attenuated in diabetic wild-type mice as compared to nondiabetic wild-type mice, diabetic and nondiabetic 4E-BP1/2–deficient mice exhibited similar SF. Although no statistical difference among strain means was observed 6 weeks post STZ, there was a trend toward lower SF in 4E-BP1/2–deficient mice ($P = 0.11$). Thus, there is tempered confidence in concluding a protective effect of 4E-BP1/2 ablation on SF, as unknown genetic variances in mouse strains with the same genetic background could also potentially contribute subtle phenotypic differences, such as the rate of SF decline in response to diabetes. The protective effect of 4E-BP1/2 ablation was principally observed in CS, which is largely associated with inner retinal information processing, as compared to the outer retina and photoreceptors. Thus, the findings herein support a role for elevated 4E-BP1 expression in the development of inner retinal dysfunction in diabetic mice. Overall, the findings suggest that the molecular mechanisms whereby altered mRNA translation in the retina contributes to visual dysfunction represent a promising target for novel therapeutics that address the development and progression of diabetic retinopathy.

Acknowledgments

The authors thank Gerald Hart, PhD (Johns Hopkins University) and the NHLBI P01HL107153 Core C4 for providing Thiamet G. The authors also thank K. Hosoya, PhD (Toyama Medical and Pharmaceutical University) for kindly providing TR-MUL cells. Finally, the authors thank Chichun E. Sun and Tony Martin for technical assistance in performance of the studies described herein.

Supported by the American Diabetes Association Pathway to Stop Diabetes Grant 1-14-INI-04 and National Institutes of Health Grants EY023612 (MDD), DK15658, and DK13499 (LSJ). The authors alone are responsible for the content and writing of the paper.

Disclosure: **W.P. Miller**, None; **M.L. Mihailescu**, None; **C. Yang**, None; **A.J. Barber**, None; **S.R. Kimball**, None; **L.S. Jefferson**, None; **M.D. Dennis,** None

References

1. Sheetz MJ, King GL. Molecular understanding of hyperglycemia's adverse effects for diabetic complications. *JAMA*. 2002; 288:2579–2588.

2. The Diabetes Control and Complications Trial Research Group. The effect of intensive treatment of diabetes on the development and progression of long-term complications in insulin-dependent diabetes mellitus. *N Engl J Med*. 1993;329:977–986.
3. Dennis MD, Kimball SR, Fort PE, Jefferson LS. Regulated in development and DNA damage 1 is necessary for hyperglycemia-induced vascular endothelial growth factor expression in the retina of diabetic rodents. *J Biol Chem*. 2015;290:3865–3874.
4. Miller JW, Adamis AP, Shima DT, et al. Vascular endothelial growth factor/vascular permeability factor is temporally and spatially correlated with ocular angiogenesis in a primate model. *Am J Pathol*. 1994;145:574–584.
5. Schrufer TL, Antonetti DA, Sonenberg N, Kimball SR, Gardner TW, Jefferson LS. Ablation of 4E-BP1/2 prevents hyperglycemia-mediated induction of VEGF expression in the rodent retina and in Muller cells in culture. *Diabetes*. 2010;59:2107–2116.
6. Ptushkina M, von der Haar T, Karim MM, Hughes JM, McCarthy JE. Repressor binding to a dorsal regulatory site traps human eIF4E in a high cap-affinity state. *EMBO J*. 1999;18:4068–4075.
7. von der Haar T, Gross JD, Wagner G, McCarthy JEG. The mRNA cap-binding protein eIF4E in post-transcriptional gene expression. *Nat Struct Mol Biol*. 2004;11:503–511.
8. Dennis MD, Shenberger JS, Stanley BA, Kimball SR, Jefferson LS. Hyperglycemia mediates a shift from cap-dependent to cap-independent translation via a 4E-BP1 dependent mechanism. *Diabetes*. 2013;62:2204–2214.
9. Wang J, Xu X, Elliott MH, Zhu M, Le YZ. Muller cell-derived VEGF is essential for diabetes-induced retinal inflammation and vascular leakage. *Diabetes*. 2010;59:2297–2305.
10. Gingras AC, Kennedy SG, O'Leary MA, Sonenberg N, Hay N. 4E-BP1, a repressor of mRNA translation, is phosphorylated and inactivated by the Akt(PKB) signaling pathway. *Genes Dev*. 1998;12:502–513.
11. Dennis MD, Schrufer TL, Bronson SK, Kimball SR, Jefferson LS. Hyperglycemia-induced O-GlcNAcylation and truncation of 4E-BP1 protein in liver of a mouse model of type 1 diabetes. *J Biol Chem*. 2011;286:34286–34297.
12. Cheng X, Hart GW. Alternative O-glycosylation/O-phosphorylation of serine-16 in murine estrogen receptor beta: post-translational regulation of turnover and transactivation activity. *J Biol Chem*. 2001;276:10570–10575.
13. Han I, Kudlow JE. Reduced O glycosylation of Sp1 is associated with increased proteasome susceptibility. *Mol Cell Biol*. 1997;17:2550–2558.
14. Zachara NE, Hart GW. O-GlcNAc modification: a nutritional sensor that modulates proteasome function. *Trends Cell Biol*. 2004;14:218–221.
15. Powers ET. Translation: an O-GlcNAc stamp of approval. *Nat Chem Biol*. 2015;11:307–308.
16. Garcia-Alai MM, Gallo M, Salame M, et al. Molecular basis for phosphorylation-dependent, PEST-mediated protein turnover. *Structure*. 2006;14:309–319.
17. Kimball SR, Horetsky RL, Jefferson LS. Implication of eIF2B rather than eIF4E in the regulation of global protein synthesis by amino acids in L6 myoblasts. *J Biol Chem*. 1998;273:30945–30953.
18. Kimball SR, Jurasinski CV, Lawrence JC Jr, Jefferson LS. Insulin stimulates protein synthesis in skeletal muscle by enhancing the association of eIF-4E and eIF-4G. *Am J Physiol*. 1997;272:C754–C759.
19. Xu Z, Wei Y, Gong J, et al. NRF2 plays a protective role in diabetic retinopathy in mice. *Diabetologia*. 2014;57:204–213.
20. Oulianova N, Falk S, Berteloot A. Two-step mechanism of phlorizin binding to the SGLT1 protein in the kidney. *J Membr Biol*. 2001;179:223–242.
21. Mizutani M, Gerhardinger C, Lorenzi M. Muller cell changes in human diabetic retinopathy. *Diabetes*. 1998;47:445–449.
22. Zhong Y, Li J, Chen Y, Wang JJ, Ratan R, Zhang SX. Activation of endoplasmic reticulum stress by hyperglycemia is essential for Muller cell-derived inflammatory cytokine production in diabetes. *Diabetes*. 2012;61:492–504.
23. Barber AJ, Antonetti DA, Gardner TW. Altered expression of retinal occludin and glial fibrillary acidic protein in experimental diabetes. The Penn State Retina Research Group. *Invest Ophthalmol Vis Sci*. 2000;41:3561–3568.
24. Rechsteiner M, Rogers SW. PEST sequences and regulation by proteolysis. *Trends Biochem Sci*. 1996;21:267–271.
25. Xu C, Kim NG, Gumbiner BM. Regulation of protein stability by GSK3 mediated phosphorylation. *Cell Cycle*. 2009;8:4032–4039.
26. Liu C, Li Y, Semenov M, et al. Control of beta-catenin phosphorylation/degradation by a dual-kinase mechanism. *Cell*. 2002;108:837–847.
27. Hart MJ, de los Santos R, Albert IN, Rubinfeld B, Polakis P. Downregulation of beta-catenin by human Axin and its association with the APC tumor suppressor, beta-catenin and GSK3 beta. *Curr Biol*. 1998;8:573–581.
28. Sutherland C. What are the bona fide GSK3 substrates? *Int J Alzheimers Dis*. 2011;2011:505607.
29. Yanagiya A, Suyama E, Adachi H, et al. Translational homeostasis via the mRNA cap-binding protein, eIF4E. *Mol Cell*. 2012;46:847–858.
30. Petroski MD, Deshaies RJ. Function and regulation of cullin-RING ubiquitin ligases. *Nat Rev Mol Cell Biol*. 2005;6:9–20.
31. Watanabe T, Mio Y, Hoshino FB, Nagamatsu S, Hirosawa K, Nakahara K. GLUT2 expression in the rat retina: localization at the apical ends of Muller cells. *Brain Res*. 1994;655:128–134.
32. Torres CR, Hart GW. Topography and polypeptide distribution of terminal N-acetylglucosamine residues on the surfaces of intact lymphocytes. Evidence for O-linked GlcNAc. *J Biol Chem*. 1984;259:3308–3317.
33. Hanover JA, Krause MW, Love DC. Bittersweet memories: linking metabolism to epigenetics through O-GlcNAcylation. *Nat Rev Mol Cell Biol*. 2012;13:312–321.
34. Guinez C, Mir AM, Dehennaut V, et al. Protein ubiquitination is modulated by O-GlcNAc glycosylation. *FASEB J*. 2008;22:2901–2911.
35. Ruan HB, Singh JP, Li MD, Wu J, Yang X. Cracking the O-GlcNAc code in metabolism. *Trends Endocrinol Metab*. 2013;24:301–309.
36. Zeidan Q, Wang Z, De Maio A, Hart GW. O-GlcNAc cycling enzymes associate with the translational machinery and modify core ribosomal proteins. *Mol Biol Cell*. 2010;21:1922–1936.
37. Liu K, Paterson AJ, Chin E, Kudlow JE. Glucose stimulates protein modification by O-linked GlcNAc in pancreatic beta cells: linkage of O-linked GlcNAc to beta cell death. *Proc Natl Acad Sci U S A*. 2000;97:2820–2825.
38. Hu P, Shimoji S, Hart GW. Site-specific interplay between O-GlcNAcylation and phosphorylation in cellular regulation. *FEBS Lett*. 2010;584:2526–2538.
39. Slawson C, Zachara NE, Vosseller K, Cheung WD, Lane MD, Hart GW. Perturbations in O-linked beta-N-acetylglucosamine protein modification cause severe defects in mitotic progression and cytokinesis. *J Biol Chem*. 2005;280:32944–32956.
40. Kettenbach AN, Schweppe DK, Faherty BK, Pechenick D, Pletnev AA, Gerber SA. Quantitative phosphoproteomics identifies substrates and functional modules of Aurora and Polo-like kinase activities in mitotic cells. *Sci Signal*. 2011;4:rs5.
41. Huttlin EL, Jedrychowski MP, Elias JE, et al. A tissue-specific atlas of mouse protein phosphorylation and expression. *Cell*. 2010;143:1174–1189.

Investigative Ophthalmology & Visual Science

42. Cantin GT, Yi W, Lu B, et al. Combining protein-based IMAC, peptide-based IMAC, and MudPIT for efficient phosphoproteomic analysis. *J Proteome Res*. 2008;7:1346–1351.
43. Wu X, Tian L, Li J, et al. Investigation of receptor interacting protein (RIP3)-dependent protein phosphorylation by quantitative phosphoproteomics. *Mol Cell Proteomics*. 2012;11:1640–1651.
44. Yu Y, Yoon SO, Poulogiannis G, et al. Phosphoproteomic analysis identifies Grb10 as an mTORC1 substrate that negatively regulates insulin signaling. *Science*. 2011;332:1322–1326.
45. Rinschen MM, Yu MJ, Wang G, et al. Quantitative phosphoproteomic analysis reveals vasopressin V2-receptor-dependent signaling pathways in renal collecting duct cells. *Proc Natl Acad Sci U S A*. 2010;107:3882–3887.
46. Shin S, Wolgamott L, Tcherkezian J, et al. Glycogen synthase kinase-3beta positively regulates protein synthesis and cell proliferation through the regulation of translation initiation factor 4E-binding protein 1. *Oncogene*. 2014;33:1690–1699.
47. Saito Y, Vandenheede JR, Cohen P. The mechanism by which epidermal growth factor inhibits glycogen synthase kinase 3 in A431 cells. *Biochem J*. 1994;303(pt 1):27–31.
48. Armstrong JL, Bonavaud SM, Toole BJ, Yeaman SJ. Regulation of glycogen synthesis by amino acids in cultured human muscle cells. *J Biol Chem*. 2001;276:952–956.
49. Fang X, Yu SX, Lu Y, Bast RC Jr, Woodgett JR, Mills GB. Phosphorylation and inactivation of glycogen synthase kinase 3 by protein kinase A. *Proc Natl Acad Sci U S A*. 2000;97:11960–11965.
50. Fang X, Yu S, Tanyi JL, Lu Y, Woodgett JR, Mills GB. Convergence of multiple signaling cascades at glycogen synthase kinase 3: Edg receptor-mediated phosphorylation and inactivation by lysophosphatidic acid through a protein kinase C-dependent intracellular pathway. *Mol Cell Biol*. 2002;22:2099–2110.
51. Way KJ, Katai N, King GL. Protein kinase C and the development of diabetic vascular complications. *Diabet Med*. 2001;18:945–959.
52. Braunstein S, Karpisheva K, Pola C, et al. A hypoxia-controlled cap-dependent to cap-independent translation switch in breast cancer. *Mol Cell*. 2007;28:501–512.
53. Avdulov S, Li S, Michalek V, et al. Activation of translation complex eIF4F is essential for the genesis and maintenance of the malignant phenotype in human mammary epithelial cells. *Cancer Cell*. 2004;5:553–563.
54. Walsh D, Mohr I. Phosphorylation of eIF4E by Mnk-1 enhances HSV-1 translation and replication in quiescent cells. *Genes Dev*. 2004;18:660–672.
55. Elia A, Constantinou C, Clemens MJ. Effects of protein phosphorylation on ubiquitination and stability of the translational inhibitor protein 4E-BP1. *Oncogene*. 2008;27:811–822.
56. Tee AR, Proud CG. DNA-damaging agents cause inactivation of translational regulators linked to mTOR signalling. *Oncogene*. 2000;19:3021–3031.
57. Braunstein S, Badura ML, Xi Q, Formenti SC, Schneider RJ. Regulation of protein synthesis by ionizing radiation. *Mol Cell Biol*. 2009;29:5645–5656.
58. Mothe-Satney I, Yang D, Fadden P, Haystead TA, Lawrence JC Jr. Multiple mechanisms control phosphorylation of PHAS-I in five (S/T)P sites that govern translational repression. *Mol Cell Biol*. 2000;20:3558–3567.

Investigative Ophthalmology & Visual Science